

# Transverse polarization of $\Lambda$ hyperons from quasi-real photoproduction on nuclei

A. Airapetian,<sup>13,16</sup> N. Akopov,<sup>27</sup> Z. Akopov,<sup>6</sup> E.C. Aschenauer,<sup>7</sup> W. Augustyniak,<sup>26</sup> R. Avakian,<sup>27</sup> A. Avetissian,<sup>27</sup> E. Avetisyan,<sup>6</sup> S. Belostotski,<sup>19</sup> N. Bianchi,<sup>11</sup> H.P. Blok,<sup>18,25</sup> A. Borissov,<sup>6</sup> J. Bowles,<sup>14</sup> I. Brodski,<sup>13</sup> V. Bryzgalov,<sup>20</sup> J. Burns,<sup>14</sup> M. Capiluppi,<sup>10</sup> G.P. Capitani,<sup>11</sup> E. Cisbani,<sup>22</sup> G. Ciullo,<sup>10</sup> M. Contalbrigo,<sup>10</sup> P.F. Dalpiaz,<sup>10</sup> W. Deconinck,<sup>6</sup> R. De Leo,<sup>2</sup> L. De Nardo,<sup>12,6</sup> E. De Sanctis,<sup>11</sup> M. Diefenthaler,<sup>15,9</sup> P. Di Nezza,<sup>11</sup> M. Düren,<sup>13</sup> M. Ehrenfried,<sup>13</sup> G. Elbakian,<sup>27</sup> F. Ellinghaus,<sup>5</sup> R. Fabbri,<sup>7</sup> A. Fantoni,<sup>11</sup> L. Felawka,<sup>23</sup> S. Frullani,<sup>22</sup> D. Gabbert,<sup>12,7</sup> G. Gapienko,<sup>20</sup> V. Gapienko,<sup>20</sup> F. Garibaldi,<sup>22</sup> G. Gavrilov,<sup>19,6,23</sup> V. Gharibyan,<sup>27</sup> F. Giordano,<sup>6,10</sup> S. Gliske,<sup>16</sup> M. Golembiovskaya,<sup>7</sup> C. Hadjidakis,<sup>11</sup> M. Hartig,<sup>6</sup> D. Hasch,<sup>11</sup> A. Hillenbrand,<sup>7</sup> M. Hoek,<sup>14</sup> Y. Holler,<sup>6</sup> I. Hristova,<sup>7</sup> Y. Imazu,<sup>24</sup> A. Ivanilov,<sup>20</sup> H.E. Jackson,<sup>1</sup> H.S. Jo,<sup>12</sup> S. Joosten,<sup>15</sup> R. Kaiser,<sup>14</sup> G. Karyan,<sup>27</sup> T. Keri,<sup>14,13</sup> E. Kinney,<sup>5</sup> A. Kisselev,<sup>19</sup> N. Kobayashi,<sup>24</sup> V. Korotkov,<sup>20</sup> V. Kozlov,<sup>17</sup> P. Kravchenko,<sup>19</sup> V.G. Krivokhijine,<sup>8</sup> L. Lagamba,<sup>2</sup> L. Lapikás,<sup>18</sup> I. Lehmann,<sup>14</sup> P. Lenisa,<sup>10</sup> A. López Ruiz,<sup>12</sup> W. Lorenzon,<sup>16</sup> X.-R. Lu,<sup>24</sup> B.-Q. Ma,<sup>3</sup> D. Mahon,<sup>14</sup> N.C.R. Makins,<sup>15</sup> S.I. Manaenkov,<sup>19</sup> Y. Mao,<sup>3</sup> B. Marianski,<sup>26</sup> A. Martinez de la Ossa,<sup>5</sup> H. Marukyan,<sup>27</sup> C.A. Miller,<sup>23</sup> Y. Miyachi,<sup>24</sup> A. Movsisyan,<sup>10,27</sup> V. Muccifora,<sup>11</sup> M. Murray,<sup>14</sup> A. Mussgiller,<sup>6,9</sup> E. Nappi,<sup>2</sup> Y. Naryshkin,<sup>19</sup> A. Nass,<sup>9</sup> M. Negodaev,<sup>7</sup> W.-D. Nowak,<sup>7</sup> L.L. Pappalardo,<sup>10</sup> R. Perez-Benito,<sup>13</sup> M. Raithel,<sup>9</sup> P.E. Reimer,<sup>1</sup> A.R. Reolon,<sup>11</sup> C. Riedl,<sup>7</sup> K. Rith,<sup>9</sup> G. Rosner,<sup>14</sup> A. Rostomyan,<sup>6</sup> J. Rubin,<sup>15</sup> D. Ryckbosch,<sup>12</sup> Y. Salomatin,<sup>20</sup> F. Sanftl,<sup>24</sup> A. Schäfer,<sup>21</sup> G. Schnell,<sup>4,12</sup> K.P. Schüller,<sup>6</sup> B. Seitz,<sup>14</sup> T.-A. Shibata,<sup>24</sup> V. Shutov,<sup>8</sup> M. Stancari,<sup>10</sup> M. Statera,<sup>10</sup> E. Steffens,<sup>9</sup> J.J.M. Steijger,<sup>18</sup> J. Stewart,<sup>7</sup> F. Stinzinger,<sup>9</sup> S. Taroian,<sup>27</sup> A. Terkulov,<sup>17</sup> R. Truty,<sup>15</sup> A. Trzcinski,<sup>26</sup> M. Tytgat,<sup>12</sup> A. Vandenbroucke,<sup>12</sup> Y. Van Haarlem,<sup>12</sup> C. Van Hulse,<sup>4,12</sup> D. Veretennikov,<sup>19</sup> V. Vikhrov,<sup>19</sup> I. Vilardi,<sup>2</sup> S. Wang,<sup>3</sup> S. Yaschenko,<sup>7,9</sup> Z. Ye,<sup>6</sup> W. Yu,<sup>13</sup> V. Zagrebelsky,<sup>13,6</sup> D. Zeiler,<sup>9</sup> B. Zihlmann,<sup>6</sup> and P. Zupranski<sup>26</sup>

(The HERMES Collaboration)

<sup>1</sup>Physics Division, Argonne National Laboratory, Argonne, Illinois 60439-4843, USA

<sup>2</sup>Istituto Nazionale di Fisica Nucleare, Sezione di Bari, 70124 Bari, Italy

<sup>3</sup>School of Physics, Peking University, Beijing 100871, China

<sup>4</sup>Department of Theoretical Physics, University of the Basque Country UPV/EHU, 48080 Bilbao, Spain and IKERBASQUE, Basque Foundation for Science, 48011 Bilbao, Spain

<sup>5</sup>Nuclear Physics Laboratory, University of Colorado, Boulder, Colorado 80309-0390, USA

<sup>6</sup>DESY, 22603 Hamburg, Germany

<sup>7</sup>DESY, 15738 Zeuthen, Germany

<sup>8</sup>Joint Institute for Nuclear Research, 141980 Dubna, Russia

<sup>9</sup>Physikalisches Institut, Universität Erlangen-Nürnberg, 91058 Erlangen, Germany

<sup>10</sup>Istituto Nazionale di Fisica Nucleare, Sezione di Ferrara and Dipartimento di Fisica e Scienze della Terra, Università di Ferrara, 44122 Ferrara, Italy

<sup>11</sup>Istituto Nazionale di Fisica Nucleare, Laboratori Nazionali di Frascati, 00044 Frascati, Italy

<sup>12</sup>Department of Physics and Astronomy, Ghent University, 9000 Gent, Belgium

<sup>13</sup>II. Physikalisches Institut, Justus-Liebig Universität Gießen, 35392 Gießen, Germany

<sup>14</sup>SUPA, School of Physics and Astronomy, University of Glasgow, Glasgow G12 8QQ, United Kingdom

<sup>15</sup>Department of Physics, University of Illinois, Urbana, Illinois 61801-3080, USA

<sup>16</sup>Randall Laboratory of Physics, University of Michigan, Ann Arbor, Michigan 48109-1040, USA

<sup>17</sup>Lebedev Physical Institute, 117924 Moscow, Russia

<sup>18</sup>National Institute for Subatomic Physics (Nikhef), 1009 DB Amsterdam, The Netherlands

<sup>19</sup>B.P. Konstantinov Petersburg Nuclear Physics Institute, Gatchina, 188300 Leningrad region, Russia

<sup>20</sup>Institute for High Energy Physics, Protvino, 142281 Moscow region, Russia

<sup>21</sup>Institut für Theoretische Physik, Universität Regensburg, 93040 Regensburg, Germany

<sup>22</sup>Istituto Nazionale di Fisica Nucleare, Sezione di Roma, Gruppo Collegato Sanità and Istituto Superiore di Sanità, 00161 Roma, Italy

<sup>23</sup>TRIUMF, Vancouver, British Columbia V6T 2A3, Canada

<sup>24</sup>Department of Physics, Tokyo Institute of Technology, Tokyo 152, Japan

<sup>25</sup>Department of Physics and Astronomy, VU University, 1081 HV Amsterdam, The Netherlands

<sup>26</sup>National Centre for Nuclear Research, 00-689 Warsaw, Poland

<sup>27</sup>Yerevan Physics Institute, 375036 Yerevan, Armenia

(Dated: June 13, 2014)

The transverse polarization of  $\Lambda$  hyperons was measured in inclusive quasi-real photoproduction for various target nuclei ranging from hydrogen to xenon. The data were obtained by the HERMES experiment at HERA using the 27.6 GeV lepton beam and nuclear gas targets internal to the lepton storage ring. The polarization observed is positive for light target nuclei and is compatible with zero for krypton and xenon.

## INTRODUCTION

Transverse polarization of  $\Lambda$  hyperons produced in inclusive unpolarized hadron-nucleon, hadron-nucleus, and nucleus-nucleus collisions at high energies is a well established phenomenon. The polarization  $P_n^\Lambda$  measured in these experiments with hadron beams is perpendicular to the production plane spanned by the momentum vectors  $\vec{k}$  and  $\vec{p}$  of the beam and the produced  $\Lambda$ , respectively, the only direction allowed by parity conservation for an axialvector quantity and unpolarized beams and targets. A substantial transverse  $\Lambda$  polarization was first observed in proton-beryllium collisions at a proton-beam energy of 300 GeV [1]. Since then, numerous experiments using a variety of beams and targets have been performed to study this effect in detail. For a review of results and experiments see, e.g., Refs. [2–4]. The polarization is essentially independent of the beam momentum; its magnitude rises with  $p_T$ , the  $\Lambda$  momentum component transverse to the beam direction, for  $p_T$  values up to about 1 GeV, where it reaches values of up to  $|P_n^\Lambda| \approx 0.4$ , then it is independent of  $p_T$  up to the highest measured  $p_T$  values of about 3 GeV. At fixed  $p_T$ ,  $P_n^\Lambda$  rises with the Feynman variable  $x_F = p_L^*/p_{L,max}^*$ , where  $p_L^*$  is the component of the  $\Lambda$  momentum in the beam direction measured in the beam-target center-of-mass system and  $p_{L,max}^*$  is its maximal possible value. The transverse polarization depends only weakly on the atomic-mass number  $A$  of the target nuclei [2, 3, 5]. No difference was observed between hydrogen (H) and deuterium (D) targets within the statistical accuracy of the measurements, whereas the polarization for beryllium appeared to be of slightly smaller magnitude than that for H and D [6]. A relative reduction of the magnitude of the polarization by about 20% was observed for copper and lead targets compared to beryllium. Furthermore,  $P_n^\Lambda$  remained small in relativistic heavy-ion collisions up to  $p_T \approx 2.5$  GeV. At higher transverse momenta,  $P_n^\Lambda$  measured in such experiments was found to be similar to that observed in p-p or p-nucleus scattering [7]. The measured polarization is negative for most of the hadron beams, i.e., the polarization vector  $\vec{P}_n^\Lambda$  and the normal  $\hat{n} = \vec{k} \times \vec{p}/|\vec{k} \times \vec{p}|$  to the production plane have opposite directions, but it is positive for  $K^-$  [8] and  $\Sigma^-$  [9] beams.

While transverse polarization of hyperons was studied in detail with hadron beams, very little experimental information about  $P_n^\Lambda$  is available from photo- or electroproduction. Early measurements [10, 11] were of low statistical accuracy. More recently, the HERMES experiment has obtained for the first time statistically significant experimental results on the transverse  $\Lambda$  polarization in inclusive quasi-real photoproduction [12]. The measured polarization is positive, the same as those observed for  $K^-$  and  $\Sigma^-$  beams.

The analysis presented in Ref. [12] combined the data

collected by the HERMES experiment in the years 1996–2000 using mostly hydrogen and deuterium targets. More data were collected in the years 2002–2005 with the target nuclei H, D,  $^4\text{He}$ , Ne, Kr, and Xe, which allowed the study of the dependence of  $P_n^\Lambda$  on the atomic-mass number  $A$  of the target nuclei. The results of all these measurements are presented here.

## EXPERIMENT

The data were accumulated by the HERMES experiment at the HERA accelerator facility of DESY. The 27.6 GeV lepton (electron or positron) beam passed through a 40 cm long open-ended tubular storage cell internal to the lepton storage ring. The storage cell was filled with polarized or unpolarized target gas of the various elements. Part of the data was collected using a transversely or longitudinally polarized hydrogen target and a longitudinally polarized deuterium target, respectively. The direction of the target polarization was reversed in 1–3 min intervals, resulting in a vanishing average target polarization of the data set.

The HERMES detector is described in detail in Ref. [13]. It was a forward magnetic spectrometer with a geometric acceptance confined to two regions in scattering angle, arranged symmetrically above (top) and below (bottom) the beam pipe and covering ranges of  $\pm(40\text{--}140)$  mrad in the vertical and  $\pm 170$  mrad in the horizontal component of the scattering angle with respect to the center of the target cell.

The criteria for data selection and the analysis procedure are similar to those described in detail in Ref. [12]. The scattered lepton was not required to be detected. In this case the data sample is dominated by the kinematic regime of quasi-real photoproduction with  $Q^2 \approx 0$  GeV<sup>2</sup>, (where  $-Q^2$  represents the squared four-momentum of the virtual photon exchanged in the electromagnetic interaction). An average energy  $\langle \nu \rangle \approx 16$  GeV of the quasi-real photons was obtained from a Monte Carlo simulation of the process using the PYTHIA event generator [14] and a GEANT [15] model of the detector.

The  $\Lambda$  events were detected through their  $\Lambda \rightarrow p\pi^-$  decay channel, by requiring the presence of at least two hadron candidates of opposite charges. In the event selection the fact was used that in the laboratory system the momentum of the decay proton is always larger than the pion momentum for  $\Lambda$  momenta above  $\sim 300$  MeV. The information from a dual-radiator ring-imaging Cherenkov counter was used to assure that the positive hadron was not a pion. When more than one positive or negative hadron was found in an event, all possible combinations of oppositely charged hadron pairs were considered. All tracks were also required to satisfy a series of fiducial-volume cuts designed to avoid the inactive edges of the detector. Furthermore, both hadron tracks were

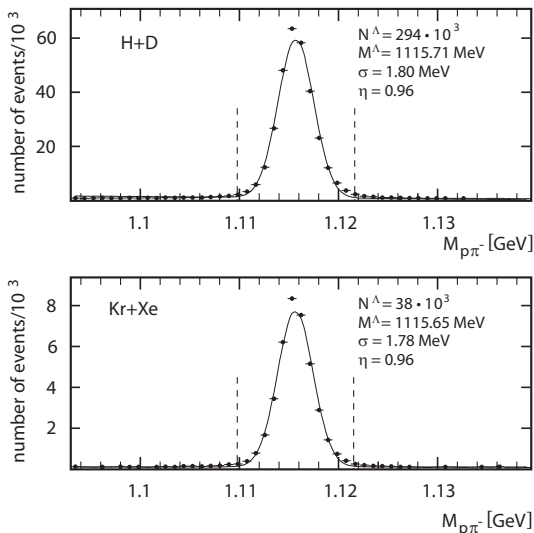


FIG. 1: Invariant-mass distributions for  $\Lambda$  events obtained with hydrogen and deuterium targets (top panel) and with krypton and xenon targets (bottom panel). The vertical lines indicate the invariant-mass interval used for the determination of the  $\Lambda$  polarization. The quantities given in the legends are: the number of analyzed  $\Lambda$  events,  $N^\Lambda$ , in the selected invariant-mass window after subtraction of background events, the reconstructed  $\Lambda$  mass  $M^\Lambda$ , the resolution  $\sigma$  of the invariant-mass distribution, and the fraction  $\eta$  of  $\Lambda$  events in this mass window.

required to be reconstructed in the same spectrometer half to avoid effects caused by possible misalignment of the two spectrometer halves relative to each other. This requirement reduced the number of  $\Lambda$ -event candidates by  $\sim 15\%$ .

Track reconstruction was performed with a track-fitting algorithm based on Kalman filter with substantially improved vertex determination and momentum resolution compared to the one used for the data published previously. This algorithm allows to give best-possible estimates on track parameters at the beam crossing and/or at the (possible) vertices with other tracks of a given event. Two spatial vertices were reconstructed for each event: the  $\Lambda$ -decay vertex from the intersection of the proton and pion tracks and the  $\Lambda$ -production vertex from the intersection of the reconstructed  $\Lambda$  track with the nominal beam axis. The  $\Lambda$ -production vertex was required to be downstream of the upstream end of the target cell and the decay vertex was required to be at least 40 cm downstream of the center of the target cell. The latter requirement was chosen as a compromise between statistical precision and low background of the data sample and the need to avoid, for data taken with a polarized target, any residual influence of the target's magnetic field on the polarization measurement.

For tracks fulfilling all above given requirements the

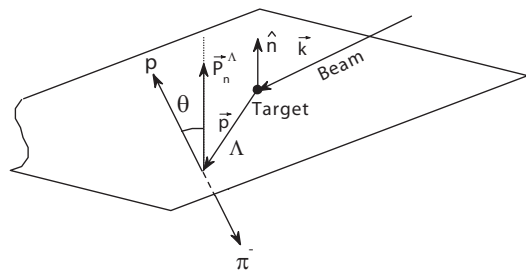


FIG. 2: Sketch of  $\Lambda$  production and decay. The polarization vector  $\vec{P}_n^\Lambda$  is directed along the normal  $\hat{n}$  to the  $\Lambda$  production plane;  $\theta$  is the angle between the momentum of the decay proton and  $\hat{n}$  in the rest frame of the  $\Lambda$  hyperon.

invariant mass of the hadron pair was evaluated. The resulting invariant-mass distributions for the combined hydrogen and deuterium (H+D) and the combined krypton and xenon (Kr+Xe) data are shown in Fig. 1. These distributions are very similar for all nuclei. They were fitted by a Gaussian plus a second order polynomial line shape. Compared to the data published previously [12], the resolution  $\sigma$  of the mass reconstruction was improved from 2.23 MeV to 1.80 MeV. The position of the  $\Lambda$  peak agrees within  $\sim 0.10$  MeV with the world average of  $(1115.683 \pm 0.006)$  MeV [16]. Events within an invariant-mass window of  $\pm 3.3\sigma$  around the mean value of the Gaussian fit were selected, and background events,  $N^{\text{bgr}}$ , were subtracted with a procedure described in Ref. [12]. The background is small, the fraction  $\eta = N^\Lambda / (N^\Lambda + N^{\text{bgr}})$  of  $\Lambda$  events in the selected mass window being  $\sim 96\%$  for all targets.

## EXTRACTION OF $\Lambda$ POLARIZATION

The topology of  $\Lambda$  production and decay is sketched in Fig. 2 where the decay into proton and pion is shown in the  $\Lambda$  rest frame. The method of extraction of the transverse  $\Lambda$  polarization is described in detail in Ref. [12]. For the parity-violating  $\Lambda \rightarrow p\pi^-$  decay, the angular distribution of the decay protons in the  $\Lambda$  rest frame is given by

$$\frac{dN}{d\Omega} = \frac{dN_0}{d\Omega} (1 + \alpha P_n^\Lambda \cos \theta), \quad (1)$$

where  $\frac{dN_0}{d\Omega}$  is the decay distribution for unpolarized  $\Lambda$  hyperons,  $\theta$  is the angle between the proton momentum and the normal  $\hat{n}$ , and  $\alpha = 0.642 \pm 0.013$  [16]. The decay protons are preferentially emitted along the spin direction of the  $\Lambda$  in its rest frame. This provides the possibility to obtain the  $\Lambda$  polarization by measuring the asymmetry in the proton's angular distribution.

For a detector with  $4\pi$  acceptance, the polarization is given by  $P_n^\Lambda = \frac{3}{\alpha} \langle \cos \theta \rangle$ , where  $\langle \cos \theta \rangle \equiv$

$\frac{1}{N^\Lambda} \sum_{i=1}^{N^\Lambda} (\cos \theta)_i$  is the first moment of the angular distribution and  $N^\Lambda$  is the number of  $\Lambda$  events analyzed. For a detector with non-uniform acceptance, the linear  $\cos \theta$  distribution in Eq. 1 can be strongly distorted. For the determination of  $P_n^\Lambda$  the mean value of  $\cos \theta$  for the *unpolarized* distribution,  $\langle \cos \theta \rangle_0$ , must be known with good precision. For a detector with ideal top/bottom mirror symmetry, there is an important simplification: the first moment for unpolarized  $\Lambda$  events vanishes ( $\langle \cos \theta \rangle_0 = 0$ ), and  $\langle \cos^m \theta \rangle_0 = \langle \cos^m \theta \rangle$  ( $m = 2, 4, \dots$ ), i.e., all even “polarized” moments are equal to the “unpolarized” ones. This allows the determination of  $P_n^\Lambda$  using only the experimentally measured values for  $(\cos \theta)_i$  without the need of a Monte Carlo simulation of the spectrometer acceptance:

$$P_n^\Lambda = \frac{\langle \cos \theta \rangle}{\alpha \langle \cos^2 \theta \rangle}. \quad (2)$$

The numerator in Eq. 2 represents the measured asymmetry in the angular distribution while the denominator stands for the analyzing power in the case of non-uniform acceptance. For the HERMES spectrometer, the top/bottom mirror symmetry is not absolutely perfect and Eq. 2 is only a good approximation. The true values for  $\langle \cos \theta \rangle_0$  and  $P_n^\Lambda$  have therefore to be determined in an iterative procedure that takes into account the measured differences between  $\langle \cos \theta \rangle$  for the top and bottom halves of the detector [12].

## RESULTS

The experimental results for the extracted transverse polarization  $P_n^\Lambda$ , averaged over all kinematic variables, are presented in Table I for the various target nuclei, together with the statistical uncertainties of the measurements, the number of  $\Lambda$  events in the selected invariant-mass window after subtraction of background events, and the fraction  $\eta$  of  $\Lambda$  events in this mass window. Also presented are the difference  $\Delta M^\Lambda$  between the reconstructed  $\Lambda$  mass and the world average [16], the resolution  $\sigma$  of the invariant-mass distribution, the average values of the transverse  $\Lambda$  momentum,  $p_T$ , and of the variable  $\zeta = (E^\Lambda + p_L)/(E + k) \approx E^\Lambda/E$ . Here  $E^\Lambda$  and  $E$  are the energies of the  $\Lambda$  produced and the beam lepton, respectively, and  $p_L$  is the  $\Lambda$ 's momentum component in the beam direction measured in the target rest frame. As discussed in Ref. [12], the variable  $\zeta$  provides an approximate measure of whether the  $\Lambda$  hyperon was produced in the forward region ( $\zeta > 0.3$ ) in the center-of-mass frame of the  $\gamma^*$ -nucleon reaction, whereas for  $\zeta < 0.2$  it is predominantly produced in the backward region but with still a significant admixture of forward going  $\Lambda$  hyperons. The values of  $\Delta M^\Lambda$ ,  $\sigma$ ,  $\langle p_T \rangle$ , and  $\langle \zeta \rangle$  are very similar for all targets.

	H	D	$^4\text{He}$	Ne	Kr	Xe
$P_n^\Lambda$	0.062	0.052	0.051	0.092	-0.005	0.010
$\delta P_n^\Lambda(\text{stat.})$	0.008	0.006	0.044	0.026	0.017	0.023
$N^\Lambda/10^3$	108.5	185.9	3.4	10.2	24.2	13.7
$\eta$	0.96	0.96	0.96	0.96	0.96	0.97
$\Delta M^\Lambda$ [MeV]	0.02	0.05	0.09	0.11	0.04	0.00
$\sigma$ [MeV]	1.79	1.82	1.96	1.89	1.77	1.79
$\langle p_T \rangle$ [GeV]	0.63	0.63	0.67	0.68	0.64	0.64
$\langle \zeta \rangle$	0.25	0.25	0.27	0.27	0.25	0.25

TABLE I: Average transverse  $\Lambda$  polarization  $P_n^\Lambda$  for various target nuclei together with the statistical uncertainties  $\delta P_n^\Lambda(\text{stat.})$  of the measurements, the number of analyzed  $\Lambda$  events,  $N^\Lambda$ , in the selected invariant-mass window after subtraction of background events, and the fraction  $\eta$  of  $\Lambda$  events in this mass window. Also presented are the difference  $\Delta M^\Lambda$  between the reconstructed  $\Lambda$  mass and the world average [16], the resolution  $\sigma$  of the invariant-mass distribution, and the average values of the the transverse  $\Lambda$  momentum  $\langle p_T \rangle$  and the variable  $\langle \zeta \rangle$ , which is an approximate measure of whether the  $\Lambda$  is produced in the forward or in the backward region (see text). The systematic uncertainty is 0.02 for all targets.

The systematic uncertainty of  $P_n^\Lambda$  has been estimated to be  $\pm 0.02$ . This value was derived from detailed Monte Carlo studies that took into account possible detector misalignments, and also from the false polarization measured for  $K_s^0 \rightarrow \pi^+\pi^-$  events that provide an event topology with two separated vertices similar to  $\Lambda$  decays. Some data were taken with a transversely polarized hydrogen target. The effects of the transversely oriented magnetic holding field in the target region were taken into account in the reconstruction of the charged-particle tracks. The integrated transverse target field was  $\sim 0.17$  Tm. This caused an average precession of the  $\Lambda$ 's magnetic moment of less than one degree, with negligible impact on the extracted transverse polarization.

The results for the measured transverse polarizations are presented in Fig. 3 as a function of the atomic-mass number  $A$  of the various target nuclei. The results for the light nuclei are significantly positive, those for hydrogen and deuterium agree within their statistical uncertainties. The average value for H+D is  $\langle P_n^\Lambda(\text{H} + \text{D}) \rangle = 0.056 \pm 0.005(\text{stat.}) \pm 0.020(\text{sys.})$  with the average value for all nuclei being  $\langle P_n^\Lambda(\text{all } A) \rangle = 0.044 \pm 0.011$ .

The transverse polarization for neon is above this value by more than one standard deviation, while the results for krypton and xenon are compatible with zero within the statistical uncertainties of the data. The average



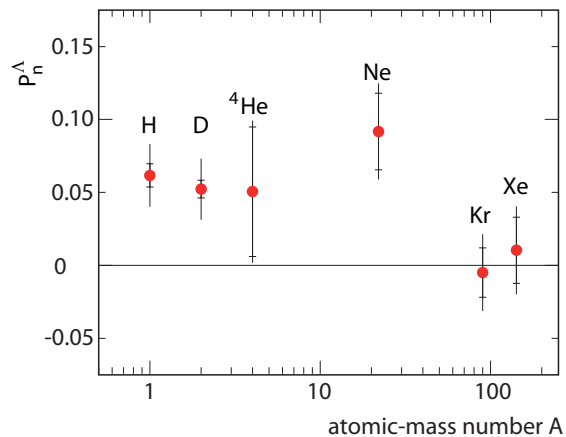


FIG. 3: Dependence of the transverse polarization  $P_n^\Lambda$  on the atomic-mass number  $A$  of the target nuclei. The inner error bars represent the statistical uncertainties; the full error bars represent the total uncertainties, evaluated as the sum in quadrature of statistical and systematic uncertainties.

value of  $P_n^\Lambda$  for the combined krypton and xenon data is  $\langle P_n^\Lambda(\text{Kr} + \text{Xe}) \rangle = 0.000 \pm 0.014(\text{stat.}) \pm 0.020(\text{sys.})$ .

Despite the rather large value for neon there is an indication of a decrease of  $P_n^\Lambda$  with the atomic-mass number  $A$  of the target nuclei. The statistical accuracy of the measurements does, however, not allow a precise determination of the functional form of this  $A$  dependence.

The  $\Lambda$  polarizations for the combined H+D and the combined Kr+Xe data are shown as a function of  $\zeta$  in Fig. 4. The H+D data (closed symbols) decrease continuously from a value of  $\sim 0.08$  at low  $\zeta$  to  $\sim 0.02$  at  $\zeta \simeq 0.45$ , while the Kr+Xe data (open symbols) fluctuate around zero. It should be noted that for each point in  $\zeta$  the average value of  $p_T$  is different as it is shown in the lower panel of the figure.

In Fig. 5 the polarizations are shown as a function of  $p_T$ . The H+D data are presented for two intervals in the variable  $\zeta$ . The  $p_T$  dependence in these two intervals is rather different. In the region  $\zeta < 0.2$ , where the produced  $\Lambda$  hyperons mainly stem from the backward region, the polarization increases linearly with  $p_T$  up to a value of  $\sim 0.12$  at  $p_T \simeq 0.75$  GeV (closed circles), while in the region  $\zeta > 0.3$  (closed squares) the polarization is substantially smaller with very little dependence on  $p_T$ . The statistical uncertainties of the Kr+Xe data prevent a firm conclusion about the  $p_T$  dependences in the two  $\zeta$  regions. The polarization is compatible with zero over the whole  $p_T$  range although the average polarisation in the region  $\zeta < 0.2$  is  $0.059 \pm 0.024(\text{stat.})$ , while it is  $-0.012 \pm 0.027(\text{stat.})$  in the region  $\zeta > 0.3$ .

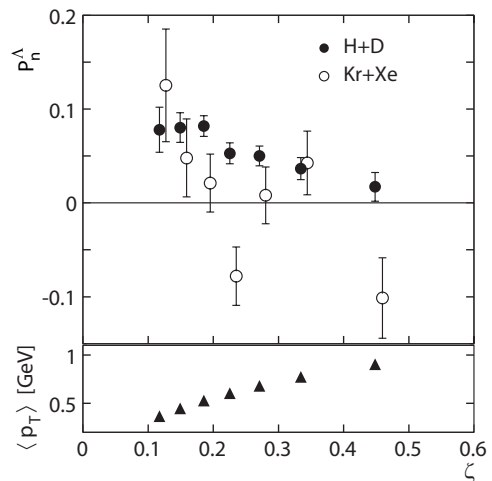


FIG. 4: Dependence of the transverse polarization  $P_n^\Lambda$  for the combined hydrogen and deuterium data (closed symbols) and the combined krypton and xenon data (open symbols) on the variable  $\zeta$ . The error bars represent statistical uncertainties only, the systematic uncertainties are not shown, since they are strongly correlated for the kinematic dependences. The values of  $\langle p_T \rangle$  for each  $\zeta$  bin are shown in the lower panel.

## DISCUSSION

Transverse  $\Lambda$  polarization  $P_n^\Lambda$  was measured in inclusive quasi-real photoproduction on nuclei. The observed polarization is positive, the same as those observed for  $K^-$  and  $\Sigma^-$  beams. There is an indication of a decrease of  $P_n^\Lambda$  with the atomic-mass number  $A$  of the target nuclei. In contrast to measurements in hadron-nucleus scattering, where the magnitude of the polarization for heavier nuclei appears to be somewhat smaller than for light nuclei but still substantially different from zero, the polarization for the combined Kr+Xe data from the present measurement is compatible with zero within the statistical uncertainties. For the combined hydrogen and deuterium data the measured polarization decreases with the variable  $\zeta$  that provides an approximate measure of whether the  $\Lambda$  hyperon was produced in the forward or in the backward region in the center-of-mass frame of the  $\gamma^*$ -nucleon reaction. For small  $\zeta$  ( $\zeta < 0.2$ ), the polarization increases linearly with  $p_T$ , whereas in the forward region ( $\zeta > 0.3$ ) the polarization is substantially smaller with very little dependence on  $p_T$ . This behavior points to a different production mechanism in the two kinematic regions. The interpretation of these observations depends on the mechanism assumed for generating the  $\Lambda$  polarization, which at present is not understood.

The situation is further complicated by the fact that a fraction of the detected  $\Lambda$  particles and their polarization originates from decays of heavier hyperons like  $\Sigma^0$ ,  $\Sigma(1385)$ , and  $\Xi$ . So far, the transverse polarization of

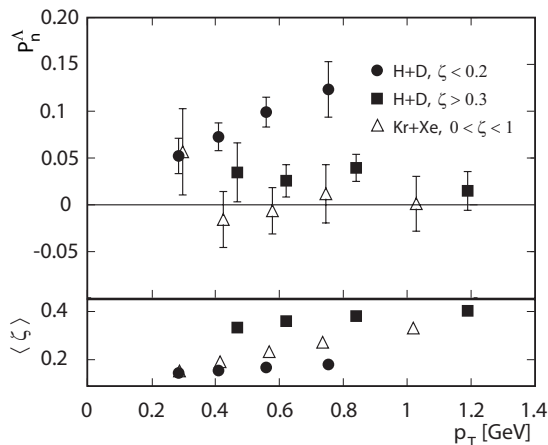


FIG. 5: Dependence of the transverse polarization  $P_n^\Lambda$  on the transverse  $\Lambda$  momentum  $p_T$ . Closed circles (squares) represent the combined hydrogen and deuterium data for the region  $\zeta < 0.2$  ( $\zeta > 0.3$ ). The combined krypton and xenon data (open triangles) are shown for the full  $\zeta$  range. The error bars represent the statistical uncertainty. The values of  $\langle \zeta \rangle$  for each  $p_T$  bin are shown in the lower panel.

these hyperons in quasi-real photoproduction is unknown as is its dependence on the nuclear target mass.

It is difficult to formulate theoretical implications of these results in general terms, i.e., without recurring to specific models. For hard processes intuitive physical pictures were proposed in the literature to explain qualitatively the origin of single-spin asymmetries (SSAs) and especially of transverse hyperon polarization, see, e.g., Refs. [4, 17, 18]. The usual factorization of QCD processes into products of distribution functions, hard amplitudes and fragmentation functions [19] requires a large momentum in the hard amplitude. This requirement is not fulfilled for quasi-real photoproduction and at the relatively small transverse momenta of the present experiment, as opposed to deep-inelastic lepton-nucleon scattering. Still, a smooth dependence on the virtuality  $Q$  of the photon would be expected such that a comparison of results from single-spin asymmetries in leptonproduction and in p+p and p+A collisions as well as corresponding theoretical calculations [20] is interesting, especially because even the sign of theoretical expectations is still under debate, see Ref. [21]. Recently, the theoretical situation seems to have been clarified by Ref. [22], which stresses that  $p_T$ -dependent fragmentation plays an important role. If so, one might also expect sizable asymmetries in soft  $p_T$ -dependent fragmentation.

#### ACKNOWLEDGEMENTS

We gratefully acknowledge the DESY management for its support and the staff at DESY and the col-

laborating institutions for their significant effort. This work was supported by the Ministry of Education and Science of Armenia; the FWO-Flanders and IWT, Belgium; the Natural Sciences and Engineering Research Council of Canada; the National Natural Science Foundation of China; the Alexander von Humboldt Stiftung, the German Bundesministerium für Bildung und Forschung (BMBF), and the Deutsche Forschungsgemeinschaft (DFG); the Italian Istituto Nazionale di Fisica Nucleare (INFN); the MEXT, JSPS, and G-COE of Japan; the Dutch Foundation for Fundamenteel Onderzoek der Materie (FOM); the Russian Academy of Science and the Russian Federal Agency for Science and Innovations; the Basque Foundation for Science (IKERBASQUE) and the UPV/EHU under program UFI 11/55; the U.K. Engineering and Physical Sciences Research Council, the Science and Technology Facilities Council, and the Scottish Universities Physics Alliance; as well as the U.S. Department of Energy (DOE) and the National Science Foundation (NSF).

- 
- [1] G. Bunce et al., Phys. Rev. Lett. 36, 1113 (1976).
  - [2] L. Pondrom, Phys. Rep. 122, 57 (1985).
  - [3] A. D. Panagiotou, Int. J. Mod. Phys. A 5, 1197 (1990).
  - [4] V. V. Abramov, Physics of Atomic Nuclei 72, 1872 (2009).
  - [5] V. M. Castillo-Vallejo and V. Gupta, Int. J. Mod. Phys. A 20, 2047 (2005).
  - [6] K. Raychaudhuri et al., Phys. Lett. B 90, 319 (1980).
  - [7] R. Bellwied et al. (E896 Collaboration), Nucl. Phys. A 698, 499 (2002).
  - [8] S. Gourlay et al., Phys. Rev. Lett. 56, 2214 (1986).
  - [9] M. I. Adamovich et al. (WA89 Collaboration), Eur. Phys. J. C 32, 221 (2004).
  - [10] D. Aston et al. (WA004 Collaboration), Nucl. Phys. B 195, 189 (1982).
  - [11] K. Abe et al. (BC072 Collaboration), Phys. Rev. D 29, 1877 (1984).
  - [12] A. Airapetian et al. (HERMES Collaboration), Phys. Rev. D 76, 092008 (2007).
  - [13] K. Ackerstaff et al. (HERMES Collaboration), Nucl. Instrum. Methods A 417, 230 (1998).
  - [14] T. Sjöstrand et al., Comput. Phys. Commun. 135, 238 (2001).
  - [15] R. Brun, R. Hagelberg, M. Hansroul, and J. C. Lassalle, CERN-DD-78-2-REV, CERN-DD-78-2.
  - [16] J. Beringer et al., Particle Data Group, Phys. Rev. D 86, 010001 (2012).
  - [17] M. Burkardt, Phys. Rev. D 66, 114005 (2002).
  - [18] B. Hannafious and M. Burkardt, PoS (LC2008) 032 (2008).
  - [19] P. J. Mulders and R. D. Tangerman, Nucl. Phys. B 461, 197 (1996); Erratum-ibid. B 484, 538 (1997).
  - [20] Y. Koike, AIP Conf. Proc. 675, 574 (2003).
  - [21] Z.-B. Kang et al., Phys. Rev. D 83, 094001 (2011).
  - [22] K. Kanazawa et al., arXiv:1404.1033 [hep-ph] (2014).